Heat Propagation Improvement in YBCO-Coated Conductors for Superconducting Fault Current Limiters

D. M. Djokić*[1], L. Antognazza[1], M. Abplanalp[2], and M. Decroux[1]
[1]Department of Quantum Matter Physics, University of Geneva, Switzerland
[2]ABB Corporate Research Center, Dättwil, Switzerland
*Corresponding author: dejan.djokic@unige.ch

Abstract: YBCO Coated Conductors (CCs), used for applications in Resistive Superconducting Fault Current Limiters (RSFCLs), are known to have insufficiently high Normal Zone Propagation Velocity (NZPV) during quench events. The improvement can be made by enhancing the thermal conductivity of YBCO-CCs with no decrease in the electrical resistivity. We studied the advantage of multi-layered structures grown on a cheap fused silica with thickness of 90 μm. The multilayer is composed of: a several microns thick copper layer to enhance the thermal conductivity, a layer to prevent the inter-diffusion, and a Hastelloy top layer. We carried out 3D FEM simulations in COMSOL Multiphysics on a meander configuration to calculate NZPV. The simulation results show a marked improvement as compared to the earlier cases [1, 2].

Keywords: Resistive Fault Current Limiters, YBCO Thin Films Applications, Cryostability of High-Temperature Superconductors, Heat Transfer and Phase Change Modelling, Medium Voltage Grids.

1. Introduction

In order to engineer superconducting cable applications, such as RSFCLs, the adequate protection from their quench damages represents one of the crucial parameters. Over the past half-century, low temperature superconductors have already proven effective in the field of cryogenic stability with reference to the operation of devices they are used for. On the other hand, high temperature superconductor applications, based on YBCO-CCs for example [3], possess quite different physical properties, with expectancy to operate within much higher temperature ranges. As their measure of cryostability, YBCO-CCs' quench propagation velocities fall into the three magnitudes lower range (of the order of cm/s) as compared to low temperature superconductors. For that reason, the use of YBCO-CCs entails high risk for damages due to eventual hot spot proliferations [4, 5]. Cabling such systems has become a subject to extensive investigations, both experimental and theoretical [6], to ensure quite a high degree of the operational stability of YBCO-CCs' devices. For example, RSFCLs made of YBCO on sapphire substrates [7] have been recognised as a possible alternative. However, these suffer from a disadvantage by virtue of their considerable costs for commercialization purposes.

In this account, our attention is devoted to numerical simulations on YBCO-CCs based RSFCLs integrated in real grid configurations. Our goal is to improve the thermal property of such superconducting devices, as well as, to optimize their designs in order to guarantee the safe integration. There are two ways of doing so: by (i) lessening the thermal influence of a massive lowermost substrate (such as SiO_2) to make the heat propagation dominated by the properties of a thermally conductive layer (such as Cu) and (ii) increasing the dimensionality up to a meander configuration. We have also raised the question of how much of the copper layer is sufficient for, in an effective sense, decoupling the YBCO-CC from the thermally inertial SiO_2. The proposed numerical model safely assumes the current transport in YBCO-CCs only and joule heating sources due to the local perturbations across the high temperature superconductor, and in the same manner, allows the variation of all the geometrical parameters relevant for the heat propagation improvement.

2. Multi-Layered Superstructure and Computational Details

We have carried out heat transfer time dependent finite element simulations in COMSOL on a simple 3D meander geometry of a novel RSFCL which is demonstrated in Figure 1. The RSFCL consists of a 40 nm Ag-coated 300 nm YBCO bonded to a multi-layered superstructure sitting

on a cheap fused silica substrate with thickness of 90 microns. The multilayer is composed of the following elements: (1) a several microns thick copper layer (varied from 0 up to 5 microns) designated to enhance the thermal conductivity of the structure, (2) a layer to prevent the inter-diffusion with (3) the Hastelloy top layer of 1 µm essential for the deposition of 2 µm thick MgO buffer layer and for avoiding the copper contamination. The realisation of the envisaged structure is well in progress [8], and yet, piloted by the simulation outcomes. Most conventionally, three experimental techniques are adopted to build up such a novel RSFCL: (1) DC magnetron sputtering system for the multilayer deposition, (2) co-evaporation technique for Ag coating and deposition growth of YBCO thin films (critical temperature T_C =92 K and critical current J_C=2 MAcm^{-2} at 77 K), and (3) ion-beam assisted deposition for bi-axially alignment of the MgO template.

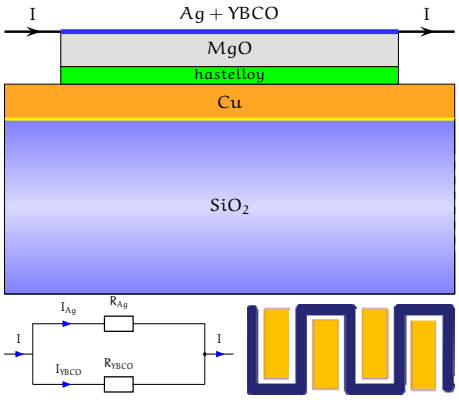

Figure 1. Novel multi-layered superstructure (upper panel) configurated into a meander geometry (down right) of an YBCO-based CC lying on the copper+SiO_2 substrate. The superconducting line is electrically isolated from the substrate so that the current is shared in YBCO-based CC only (down left).

Without loss of generality, the simulated geometry of the meander (Fig. 1 down right panel) has been streamlined to comprise only three superconducting lines (each 6 mm×20 mm), separated by 0.4 mm lying on the top of the copper layer. The entire configuration is immersed into a thermal bath of liquid nitrogen (77 K). The dissipation initialization is achieved by locally weakening the critical current density. Therefore, the central 6 mm × 50 µm block (T_C=92 K and J^B_C=0.1 MAcm^{-2}) of the middle line (Fig. 2) is taken to be in the normal state even well below 92 K and represents the T-J dependent heat source which is, accordingly, time dependent too. Once a DC current is switched on, the initial normal block, as a hot spot naturally existing in such systems [5], is gradually spreading along the line like an avalanche due to the assisted superconducting transition. The operational current is shared in the Ag-coated YBCO layer only (Fig. 1 down left panel) with its constant density of J=2.5 MAcm^{-2}. Although, the realistic RSFCL applications are designed for current limitations in AC networks, the typical thermal times of both diffusive and superconducting transition assisted heat propagations [9] are much shorter than common AC periods (25 ms for 50 Hz), as will be verified later in the text. Because of computational convergence issues on one hand side and meshing distribution on the other, the size of the normal block has been cautiously tuned to ultimately yield an optimal length of 50 µm for the present case [1].

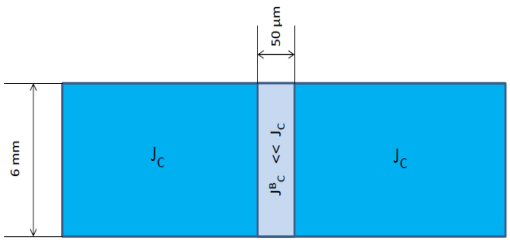

Figure 2. A scetch of the central 6 mm × 50 µm block with the critical current much lower as compared to the reamaing superconductiong parts. The block is extremely resistive even at 77 K for operational currents of 1 MAcm^{-2}.

As a heat source input, the T-J dependent power density function (Fig. 4) has been evaluated numerically in R based on the so-called current sharing function (Fig. 3). Observing the complexity of the problem with regards to mixing instantaneously temperature and current dependencies of YBCO resistivity, the solution in the circuit element (Fig. 1 down left panel) has been achieved self-constituently with several short time consuming loops. It assumes the following temperature dependent form of the YBCO flux flow resistivity which can be encountered elsewhere [10]:

$$\rho(J,T)=\rho_0\cdot\left(\frac{J}{J_c(T)}-1\right)^n,\ with\ J_c(T)=J_{c0}\cdot\left(1-\frac{T}{T_c}\right)^{1/2}\cdot\left\{1-\left(\frac{T}{T_c}\right)^4\right\}^{1/2}$$

where, ρ_0 is the equivalent resistivity at $2J_C$ and n stands for the order of the power law. The two parameters must fit the properties of the superconductor for a given underlying substrate. J_{C0} represents the critical current predicted at 0 K in the self-field and it is deduced from the J_C measurement at 77 K. The size of the circuit element for current sharing has been adjusted automatically in COMSOL to the optimised meshing element distribution. There has been therefore no need for block fragmentation of the coated conductor as was an earlier computationally rather time consuming approach [1, 2].

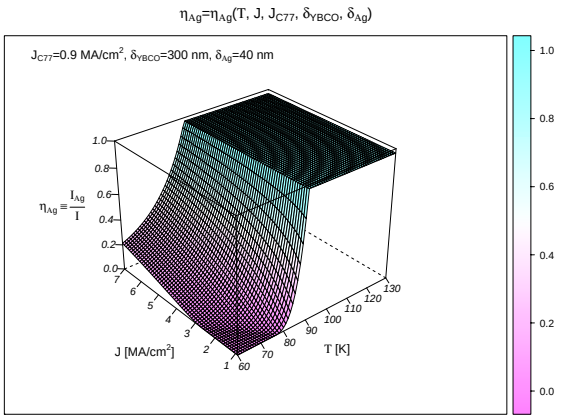

Figure 3. T-J dependent complex current sharing function reaching the plateau of height 1 above 92 K.

Finite element meshing was used to discretize the material distribution. Still, the major difficulty of the treated geometry lies in its extremely high aspect ratio that can be a challenge for an automatic or unstructured meshing where the goal is to create an isotropic mesh distribution for high mesh quality. The strategy was to subdivide the geometry into material layers with respect to the central normal block. A mapped mesh was then created on all the boundaries and distributed on the edges and peripheries. By symmetry, only one fourth of the model was simulated to speed up the computation. Thus, the symmetry boundaries were considered as nothing but the external boundaries in such a shrunken geometry.

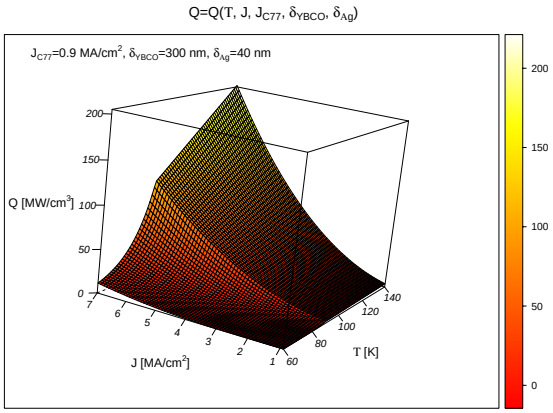

Figure 4. T-J dependent complex heat source function directly imparted from the current sharing function.

The material properties data for thermal conductivity, specific heat capacity, and convection heat transfer coefficient, all the three being isotropic and temperature dependent, were adopted from [1, 2]. The spatial dependence of YBCO resistivity along the line was not considered directly. Namely, it was incorporated implicitly through J_C spatial dependence that has a sudden drop at the position of the normal block which is a solely new layer of the same material. As with the thermal contact between the superconducting lines and the underlying multi-structure, the equivalent interface conductance was guessed from experimental results for similar structures based on a novel characterization method reported in [11]. The estimated value was taken to be 300 W $K^{-1}cm^{-2}$. For further details with regards to a discussion on the equivalent interface conductance the reader is kindly referred to [1].

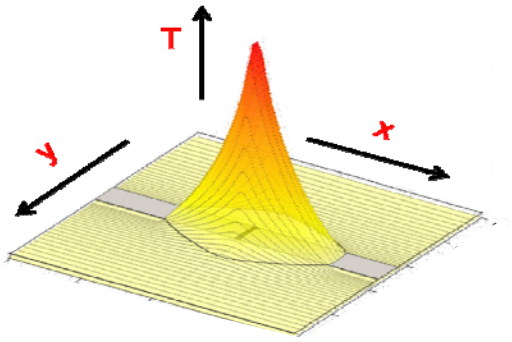

Figure 5. A temperature profile featuring longitudinal (x) and lateral (y) normal zone propagation across a single line sitting on a substrate. The figure is partially borrowed from [1].

The simulations were not of real-time type and were terminated as soon as the transition had spread out over the entire superconducting volume. Such moments were translated into real times (t_{final}) which regularly took shorter than a millisecond. Until t_{final} is reached, the average temperature of the normal block, T_{block}, was followed in order to quantity the high temperature operationality of the RSFCL. Admissible temperatures are supposed to be lower than 600 K [12] for that purpose. The heat propagation was also monitored through other referential points in time (i.e. temperature) evolution, such as: t_{trans} which represents the moment of the very first 92 K transition occurred within the normal block, and t_{600} which measures the time interval until T_{block} reaches 600 K, provided it does. Directional heat propagations along the line (longitudinal, x-axis) and sidewise (lateral, y-axis) were surveyed too (Fig. 5), with particular reference to propagating fronts of T_{NZ}=92 K, the so-called normal zones. Apart from several initial microseconds, all the values for NZPVs in the two directions of interest were found uniform over the whole interval. This is in accordance with the picture of superconducting transition assisted heat propagation [8]. The character of such a type of heat propagation is prevailing in the y-direction too knowing that the lateral NZPV is averaged out over the narrow space of the underlying layer favouring diffusive-like transport and fairly larger space of the adjacent superconducting line. Leading contributions of the diffusive-like propagations would be expected at, if of interest, larger distances between the lines.

Generally, the NZPV is a function of both J and J_C for a given substrate. However, rather than looking at the dependence with respect to these variables individually, one is usually interested in scaling the NZPV dependence down to the universal parameter J/J_C. With its values falling into the range between 1 and 1.5, it generates no extensive heating during the quench propagations. Our case is concerned with J/J_C=1.25 and can be considered rationally safe in connection with the issues with rapidly overheated RSFCLs.

The 3D model has even allowed an observation, yet only qualitative, of the heat penetration into the substrate along z-axis within few first microseconds. All the relevant times were measured from the moment the hot spot proliferation had been launched at.

3. Results and Discussions

This section is devoted to a discussion on the FEM computational results which are presented in Table 1 and obtained for the following parameters: δ_{Ag}=40 nm, δ_{YBCO}=300 nm, δ_{MgO}= 2 μm, δ_{Hast}=1 μm, δ_{Cu}=0.5-5 μm, δ_{SiO2}=90 μm, J_C=2 MAcm^{-2}, J=2.5 MAcm^{-2}, and K_{inter}=300 WK^{-1}cm^{-2}. To ensure the reliability of the simulations, the model has been successfully validated with available experimental data for both 500 μm thick sapphire and 90 μm thick hastelloy substrate; the former with J_C=3 MAcm^{-2} and J=4.5 MAcm^{-2}, while the latter with J_C=0.9 MAcm^{-2} and J=1 MAcm^{-2}. The computed values for the relevant times and temperatures were distilled directly from the COMSOL consoles, whereas the values for NZPVs were calculated based on the first derivative conditions for the normal zone time propagating path averaged along a desired direction. These conditions vary from one spatial coordinate to another depending on the mesh element distribution. The problem boils down to solving a numerical equation with respect to x for which $T(x) = T_{NZ}$. One way of doing so, that has turned out to be extremely straightforward in COMSOL, is to evaluate the expected value of the spatial coordinate $\langle x(t) \rangle$ along the line ($0<x<L$, for example) using an

integration method. It consists in centring a Gaussian density distribution peak on $T(x) = T_{NZ}$ (Fig. 6) to guarantee the highest probability for events satisfying $T(x) = T_{NZ}$. The NZPV therefore reads as follows:

$$\upsilon_{NZP} = \frac{\partial}{\partial t} \frac{\int_{x=0}^{L} x\, e^{\frac{(T(x)-T_{NZ})^2}{2\delta^2}} dx}{\left(\varepsilon + \int_{x=0}^{L} e^{\frac{(T(x)-T_{NZ})^2}{2\delta^2}} dx\right)}$$

Other solutions, however lying in the close vicinity, are weighted with less significant fractions to the integration which fall off along the Gaussian tail. Their contributions are limited due to the line-width of the Gaussian density function (δ_T) which is further controlled with the size of the projected mesh element (h) in order to provide a satisfactory smoothness of generated <x(t)> function. Ideally, the case $\delta_T=0$ would represent the exact analytical solution that can be treated in none of FEM software because of the hypothesised mesh fragmentation. The confidence intervals varied with respect to the integration direction, as well as, the available space for the integration. One must bear in mind that L_x=20 mm (length of the line), while L_y=0.4 mm (space between the lines). Such an evidently anisotropic ratio in geometry necessarily leads to the difference in relative errors for NZPV values along x, i.e. y, such that they are of 1 %, i.e. 7 %, respectively. In addition, we do not place our confidence in lateral NZPV values given that such propagations are rather of diffusive nature that may entail time dependence. Nevertheless, the order of the magnitude for lateral NZPVs appears very sensible with reference to the values for longitudinal ones.

As is shown in Figure 6, the idea of properly using the integration as a reliable NZPV calculation tool lies in covering as large number of mesh elements as possible, provided that T(x) remains a smooth function over a domain of the mesh elements. Our simplification, without loss of generality however, was to guess the linearity over one such domain that has led to the following condition: $h \times T_x' << \delta_T << T_{NZ}$, where T_x' represents the slope of T(x). A thorough description of the introduced condition is delineated in Figure 6.

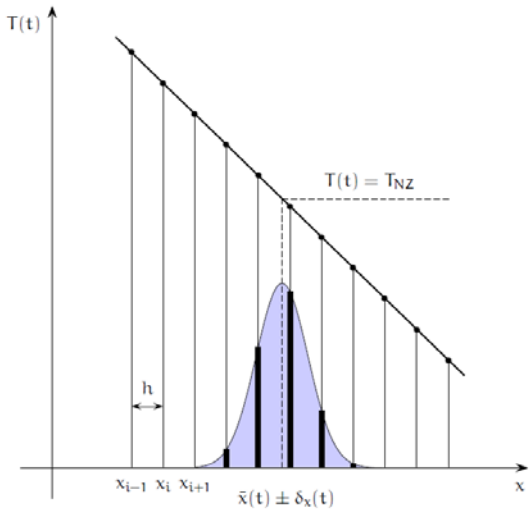

Figure 6. NZPV smoothness condition, $h << \delta_T/T_x'$, controlling the mesh size element. T(x) is guessed linear over a domain containing a large enough number of the mesh elements.

The integration runs some risk of containing division by zero. This can be escaped by inserting ϵ as an internal COMSOL constant that is a very small number of the order of 10^{-15}. Yet, one should use the *nojac* operator in COMSOL to make sure that the operating expression is excluded from the Jacobian computation. This is useful in the present case as the Jacobian contribution is not strictly necessary and the computational requirements for it are considerably high.

δ_{Cu} [μm]	0.5	1	2	3	4	5
υ_x [m/s]	3.5	4.50	4.60	4.65	4.70	4.70
υ_y [m/s]	3.5	4.0	4.0	4.0	4.1	4.1
t_{fin} [μs]	900	840	850	870	880	890
t_{trans} [μs]	40	25	30	43	55	72
t_{600} [μs]	$>t_{fin}$	$>t_{fin}$	$>t_{fin}$	$>t_{fin}$	$>t_{fin}$	$>t_{fin}$
T_{block} [K]	590	540	540	500	520	500

Table 1. The longitudinal (υ_x) and lateral (υ_y) NZPV values, relevant time parameters, and T_{block} with respect to the Cu thickness varied (δ_{Cu}). J=2.5 MAcm^{-2} and J/J_C=1.25.

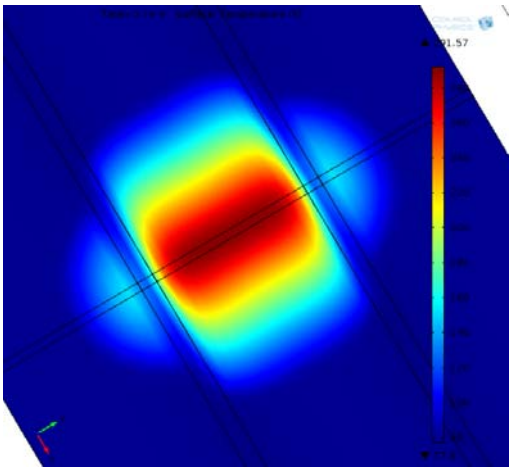

Figure 7. Temperature profile for the three superconducting lines (δ_{Cu}=2 μm) measured at 340 μs after the transition (30 μs).

The NZPV values are found quite level-headed if compared with far 13 cm/s for hastelloy and close 10 m/s for sapphire substrate at J/J_C=1.25 [12]. It is also worth noting here that this comparison is made at the fixed value of J/J_C which is the most relevant parameter for the evaluation of heat propagations in different systems. However, the complete validation of the model for the multi-structure in question is still well under way [8]. In such a manner, reconciliation can be effected between the low cost commercialisation as the strongest feature of the former and fast quench propagation as the most appealing property of the latter. For that reason one must adjust the thickness of the copper layer in order to optimize, on one hand, the influence of the underlying fused silica substrate of which 90 microns of thermal inertia may well moderate the quench propagation, and miniscule but still present thermal inertia coming from the copper itself, on the other. Saturation in the NZPV values with respect to copper thickness variation is therefore expected, as is implied from Table 1.

It is worth mentioning that there are also FEM measurements made for copper substrates thinner than 0.5 μm down to zero. It has been found that a substantial drop in the NZPV values occurs below 100 nm at which they fall in the range of the order of 10 cm/s (7 cm/s for 0 μm). The errors in the simulation measurements for such thin layers are considerably large if one bears in mind the difficulty with the mesh quality due to the extremely high aspect ratio. Nevertheless, it is of experimental interest to study only those copper layers which are thicker than a micron since acquiring the reliable experimental data on the effective thermal conductivity may become troublesome for thinner copper layers. As a result, a deposition of one up to two microns at most of copper layer would prove quite sufficient for the desirable heat propagation improvement in the proposed structure.

As with the remaining computed values at δ_{Cu}>0.5 μm, t_{trans} and t_{fin} are both found corroborative with the behaviour of the NZPVs. t_{trans} should increase with the increase of thickness of a good thermal conductor such as copper because the system gains some tendency to become robust towards the very first transition. On the other hand, t_{final} was measured as a time for which the point with the lowest temperature reaches 92 K. This point may not be kept at the same position as the copper thickness is varied. For that reason, this parameter is not quite corresponding to the time for which the normal zone extents over the entire system. Nevertheless roughly speaking, according to the relevant spatial dimensions and NZPV values, t_{final} is supposed to be of the order of 10^3 μs or less that is the case in the treated coated conductor. The thorough discussion above does not apply for δ_{Cu}<1 μm since this case starts to extend the influence of the fused silica.

In addition, none of the t_{600} values could be measured for all the six copper thicknesses as it goes beyond t_{fin} values. This further ensures the operationality of the studied RSFCL device. The heat propagation is desirably homogenised over the system upon a quench initialisation, before any eventual severe damage is inflicted [13]. That is, T_{block} as the highest temperature has always been found to be below 600 K for finite Cu thicknesses.

An example of the COMSOL temperature surface plot of the propagating normal zone over the three superconducting lines for 2 μm thick copper layer is given in Figure 7. One can delineate a 92 K border line of the propagating profile, which roughly demarcates dark blue from light blue area, at the moment when the hot

spot reaches 292 K. There is substantial heat diffusion sidewise the middle line that to some extent softens the temperature profile. Such extra temperature distribution has, however, led to no significant difference between the longitudinal NZPVs computed in 2 and 3D.

4. Concluding Remarks

In conclusion, the present computational work has made a valuable contribution to the development of superconducting high current cables with YBCO coated conductors that can be used for medium voltage power applications. The FEM model, which we have developed in COMSOL Heat Transfer Module, has been found quite accurate to simulate the 3D transition-induced heat propagation in YBCO-based CCs used for RSFCLs with simple meander geometry on a novel multi-structure (on-going experiment [8]). The computational results, which are given in the present study, have been employed to optimally moderate the experimental assortment of both thermally conductive and single crystalline substrates down to the use of copper. We have demonstrated that varying the Cu-substrate thickness above 0.5 μm has no considerable impact on longitudinal/lateral NZPVs. This means that a copper layer not thicker than a micron is sufficient to come up with an already desirable degree of the RSFCL operationality. The obtained NZPV values have proven to fall into the almost two magnitude higher range as compared to the earlier studies [2] that is promising for commercialization purposes.

5. References

[1] A. Badel, L. Antognazza, M. Therasse, M. Abplanalp, C. Schacherer, and M. Decroux, Hybrid Model of Quench Propagation in Coated Conductors for Fault Current Limiters, *Supercond. Sci. Technol.* **25**, 095015 (2012).

[2] A. Badel, L. Antognazza, M. Decroux, and M. Abplanalp, Hybrid Model of Quench Propagation in Coated Conductors Applied to Fault Current Limiter Design, *IEEE Trans. Appl. Supercond.* **23**, 5603705 (2013).

[3] J. D. Hodge, H. Muller, D. S. Applegate, and Q. Huang, A Resistive Fault Current Limiter Based on High Temperature Superconductors, *Appl. Superconductivity* **3**, 469 (1995).

[4] A. Gurevich, Thermal Instability Near Planar Defects in Superconductors, *Appl. Phys. Lett.* **78**, 1891 (2001).

[5] B. Shapiroa, G. Bela, B. Rosensteinb, and I. Shapiroa, Hot Spot in Type-II Superconductors Dynamics and Instabilities, *Physica C: Superconductivity* **404**, 335 (2004).

[6] Y. Wang, *Fundamental Elements of Applied Superconductivity in Electrical Engineering*, John Wiley & Sons, Singapore (2013).

[7] J. Duron, F. Grilli, L. Antognazza, M. Decroux, B. Dutoit, and Ø. Fischer, Finite Element Modelling of YBCO Fault Current Limiter with Temperature Dependent Parameters, *Supercond. Sci. Technol.* **20**, 338 (2007).

[8] D. M. Djokić, L. Antognazza, M. Abplanalp, and M. Decroux, *in preparation* (2014).

[9] D. M. Djokić, L. Antognazza, M. Abplanalp, and M. Decroux, Improved Heat Propagation in Coated Superconducting Fault Current Limiters, *EuCAS Conference Poster*, Genoa (2013).

[10] L. Dresner, *Stability of Superconductors*, Kluwer Academic Publishers, New York (2002).

[11] L. Antognazza, M. Decroux, A. Badel, C. Schacherer, and M. Abplanalp, Measurement of the DyBCO Substrate Thermal Conductance in Coated Conductors, *Supercond. Sci. Technol*. **25**, 105002 (2012).

[12] L. Antognazza, M. Decroux, S. Reymond, E. de Chambrier, J. M. Triscone, W. Paul, M. Chen, Ø. Fischer, Simulation of the Behaviour of Superconducting YBCO Lines at High Current Densities, *Physica C* **372–376**, 1684 (2002).

[13] M. Schwarz, C. Schacherer, K. P. Weiss, and A. Jung, Thermodynamic Behaviour of a Coated Conductor for Currents Above I_C, *Supercond. Sci. Technol*. **21**, 054008 (2008).

6. Acknowledgements

This work is supported by the National Center of Competence in Research (MaNEP, Switzerland). The assistance from Zürich COMSOL Multiphysics team, Zoran Vidaković in particular, is gratefully acknowledged.